JOURNAL OF THERMOPHYSICS AND HEAT TRANSFER
Vol. 22, No. 4, October–December 2008

Design of a Dual Latent Heat Sink for Pulsed Electronic Systems

Krishna M. Kota,* Louis C. Chow,† Jianhua Du,‡ and Jayanta S. Kapat§
University of Central Florida, Orlando, Florida 32816-2450
Quinn Leland¶
U.S. Air Force Research Laboratory, Wright–Patterson Air Force Base, Ohio 45433
and
Richard Harris**
University of Dayton Research Institute, Dayton, Ohio 45469

DOI: 10.2514/1.34998

A conceptual design of a dual latent heat sink basically intended for low thermal duty cycle electronic heat sink applications is presented. In addition to the concept, end-application-dependent criteria to select an optimized design for this dual latent heat sink are presented. A thermal resistance model has been developed to analyze and optimize the design, which would also serve as a fast design tool for experiments. The model showed that it is possible to have a dual latent heat sink design capable of handling 7 MJ of thermal load at a heat flux of 500 W/cm^2 (over an area of 100 cm^2) with a volume of 0.072 m^3 and a weight of about 57.5 kg. It was also found that, with such high heat flux absorption capability, the proposed conceptual design can have a vapor-to-condenser temperature difference of less than 10°C with a volume storage density of 97 MJ/m^3 and a mass storage density of 0.122 MJ/kg.

Nomenclature

A_H	=	area of the heat source, cm^2
a	=	vapor chamber long side, m
b	=	vapor chamber short side, m
D	=	thermal duty cycle
g	=	acceleration due to gravity, m/s^2
h_{lv}	=	latent heat of vaporization, J/kg
k_{air}	=	thermal conductivity of air, $W/m \cdot K$
k_b	=	thermal conductivity of the bond/epoxy filling the contact air gap, $W/m \cdot K$
k_{eff}	=	effective thermal conductivity of the foam and PCM composite, $W/m \cdot K$
k_{foam}	=	thermal conductivity of the foam ligaments, $W/m \cdot K$
k_l	=	thermal conductivity of the working fluid in liquid state, $W/m \cdot K$
k_{PCM}	=	thermal conductivity of phase change material, $W/m \cdot K$
M	=	molecular weight of the working fluid
m_{PCM}	=	total mass of phase change material present in the vapor chamber—thermal energy storage system, kg
m_{tot}	=	total mass of vapor chamber—thermal energy storage heat sink, kg
N	=	Boolean NO
n	=	number of columns
P_{sat}	=	normal pressure (gauge)/vapor saturation pressure, atm; P
p	=	ratio of total mass of phase change material to the total mass of the vapor chamber—thermal energy storage expressed as a percentage
pc	=	assumed critical value for the ratio of total phase change material mass to total vapor chamber—thermal energy storage mass expressed as a percentage
Q	=	total heat absorption capacity of the vapor chamber—thermal energy storage heat sink, MJ
Q_m	=	heat storage capacity per unit mass, MJ/kg
Q_v	=	heat storage capacity per unit volume, MJ/m3
q_C	=	heat flux on the condenser, W/cm^2
q_{colf}	=	column maximum heat flux absorption capability with foam inside columns, W/cm^2
q_H	=	heat flux from the heater, W/cm^2
q_i	=	heat flux on each column, W/cm^2
R_u	=	universal gas constant, $J/kg \cdot K$
r	=	ratio of used phase change material mass to the total phase change material mass expressed as a percentage
rc	=	assumed critical value for the ratio of used phase change material mass to the total phase change material mass expressed as a percentage
T_C	=	Condenser surface temperature, K
T_H	=	heater surface temperature, K
T_{PCM}	=	phase change material temperature, K
T_{sat}	=	actual value of vapor saturation temperature, K
T_v	=	guess value of vapor saturation temperature, K
T_{wall}	=	column outside wall (on the vapor side) temperature, K
t	=	pulse heat load on time, s
t_{air}	=	thickness of the air gap, m
t_b	=	thickness of a thermal conductive bond/epoxy filling the contact air gap, m
t_c	=	vapor chamber plate thickness, mm
t_{wall}	=	column wall thickness, mm
U	=	set of initial guess variables
V	=	result set
v_{lv}	=	specific volume change during phase change, m^3/kg
x	=	length of the thermal energy storage column, m

Presented as Paper 4271 at the 39th AIAA Thermophysics Conference, Miami, FL, 25–28 June 2007; received 5 October 2007; revision received 21 April 2008; accepted for publication 29 April 2008.

*Student, Department of Mechanical, Materials and Aerospace Engineering. Member AIAA.
†Professor and University Chair, Department of Mechanical, Materials and Aerospace Engineering. Associate Fellow AIAA.
‡Research Professor, Department of Mechanical, Materials and Aerospace Engineering.
§Lockheed Martin Professor, Department of Mechanical, Materials and Aerospace Engineering. Associate Fellow AIAA.
¶Senior Mechanical Engineer.
**Research Engineer.

Y = Boolean YES
y = width of the thermal energy storage column, mm
z = height of the thermal energy storage column, m
ΔTc_{VC} = assumed critical temperature difference between vapor and condenser, K
ΔT_{PCMC} = temperature difference between phase change material and condenser surface, K
ΔT_{VC} = temperature difference between vapor and condenser, K
ΔT_{VPCM} = temperature difference between vapor and phase change material, K
ε = foam porosity
μ_l = viscosity of the working fluid in liquid state, Pa · s
ν = Poisson's ratio for the vapor chamber material
ρ_l = density of the working fluid in liquid state, kg/m^3
ρ_v = density of the working fluid in vapor state, kg/m^3
σ = accommodation coefficient
σ_{max} = maximum stress developed in any of the vapor chamber walls, MPa
σ_y = yield strength of the vapor chamber material, MPa

I. Introduction

FUTURE electronic systems will involve small size, lightweight, and compact components that release very high waste heat in a pulse. The miniaturization of such systems will generate large heat fluxes during the pulse time, which will require the development of an efficient thermal management system.

A key design issue is the need for fast charging so as not to overheat the pulse heat generating electronic device. In conventional passive latent heat sinks employing either thermal energy storage (TES) using phase change materials or using the heat pipe phenomenon, the heat transfer path composed of heat absorption, storage, and discharge will have either a high thermal resistance or a low rate of heat transfer. For instance, a latent solid–liquid phase change TES facility, if employed as a heat sink, cannot provide for rapid heat absorption because most of the available phase change materials have extremely low thermal conductivities. The inability of the heat sink to quickly absorb heat from the heat source would result in a rapid temperature rise of the heat source material and thus an eventual cessation of function. This degradation of the performance of the heat source or component being cooled will be even faster if the heat fluxes that it generates are very high. Hence, most of the latent TES devices employing phase change materials are designed as heat spreaders with a large size both at the heat absorption end and at the heat dissipation end. Low thermal conductivities of phase change materials also hamper the swiftness of heat storage in solid–liquid phase change heat storage facilities. The liquid–vapor latent phase change heat sinks, like heat pipes, always have the limitations of critical heat flux of the working fluid and evaporator dry out at high heat fluxes.

Suggestions were made by previous researchers to improve the rapidity of the heat storage process in solid–liquid phase change heat sinks and successful attempts have been made along those lines. Some of them include using fins and metal [1] or graphite [2] foams along with a phase change material (PCM) enclosed in a container or mixing highly thermal conductive metal particles or adding liquid metal to the phase change material to form a colloidal suspension [1]. Of these, employing porous graphite foam to enhance the heat transfer of a TES system proved to be very effective and successful [2].

This paper presents the concept of a dual latent heat sink basically intended for low thermal duty cycle, high heat flux electronic heat sink applications. This new heat sink design combines the features of a vapor chamber with rapid thermal energy storage employing graphite foam inside the heat storage facility along with phase change materials. Instead of using a heat pipe for heat absorption, a vapor chamber acting as a heat spreader enables more uniform temperature distribution along the surface of the device being cooled, yet still incorporates the rapid heat absorption feature of a heat pipe. Hence, the vapor chamber feature elevates the system thermal conductivity by about hundred to thousand times that of pure metallic copper. This feature coupled with the rapid TES facility in the design makes this integrated system an interesting and useful one for multiple thermal management applications. The main focus of this work is to use phase change materials as a temporary storage of waste heat for heat sink applications. The reason for storing the high heat fluxes temporarily is to be able to reject the heat at the average level when the heat source is off. If heat has to be rejected in real time, the condenser has to be very large. The current design incorporates all the attractive features, such as fast charging ability for moderate-to-high heat fluxes, compactness, reliability, and light weight.

Potential application areas include, but are not limited to, temperature control of insulated gate bipolar transistors and metal–oxide-semiconductor field-effect transistors, electronic cooling in aircraft and avionics, intermittent high-speed machine element cooling, high-speed laser component cooling, high-power microwave and missile launch applications, and, more typically, thermal management in directed-energy weapon systems.

Few works dealing with an integrated vapor chamber and a thermal energy storage system have been reported in the open literature. The configuration studied by Chang et al. [3] was similar, but was composed of an axially grooved heat pipe incorporated with TES to mitigate pulse heat loads. Some of the previous attempts regarding dual latent heat sinks were reported in [4–17]. For example, in [9], a heat pipe was used to transfer heat from a solar panel and then store it in a PCM for temperature control of buildings. In [10], a unidirectional heat pipe was coupled with a PCM lying outside of it, and its key motive for using PCM is for the temporary absorption of heat during reversal environmental conditions outside the heat sink system. Cao [11] mentioned the idea of using a heat pipe to transfer heat from the human body to a chunk of PCM lying outside the heat pipe. Giammaruti [12] discussed the concept of using PCM as an interface between a hot object and a heat pipe. Glover et al. [13] proposed using a heat pipe as an auxiliary unit for a TES unit or in conjunction with the TES unit by its side for the thermal management of electronics in a closed housing. Lin et al. [14] proposed using PCMs in parallel operation with an oscillating heat pipe to absorb heat from an electromechanical actuator. In [15], PCMs were proposed for use outside a heat pipe to store excess heat emanating from a laptop computer. The novelty of the current concept lies in using a PCM for TES inside a vapor chamber (thereby tremendously increasing the condensation area for vapor) and thus coupling both the features, rather than simply using TES and a vapor chamber as separate entities in series or in parallel. In some known heat sinks [5,16] composed of PCM-encapsulated spheres lying inside a heat pipe, a good heat conducting path does not exist between the PCM-encapsulated spheres (because of point-to-point contacts that exist between clusters of spheres and the low thermal conductivity of the sphere materials) during discharging. In addition, no thermal conductivity enhancement mechanism was used in any of the previous similar attempts. Other key improvements in the current design (that have not been attempted before) are elucidated in a detailed manner in the section on design considerations.

The basic goal of the paper is to show by theoretical modeling and optimization that this concept is feasible and can have a very low vapor-to-condenser temperature difference along with a high heat flux absorption capability.

II. Concept of Integrated Vapor Chamber—Thermal Energy Storage System

Figure 1 shows the concept of the integrated vapor chamber—thermal energy storage (VCTES) system used as a heat sink in a spray cooling application. It consists of a solid container with a liquid–vapor phase change conducting fluid/heat transfer fluid (HTF). Columns/containers, which are adequately spaced, are attached to the top of the container and encapsulate a phase change material for thermal energy storage.

When the heat load is on, the working fluid in the spray cooling chamber (or any other heat source) absorbs the heat and changes its phase from liquid to vapor and the vapor spreads in the VCTES

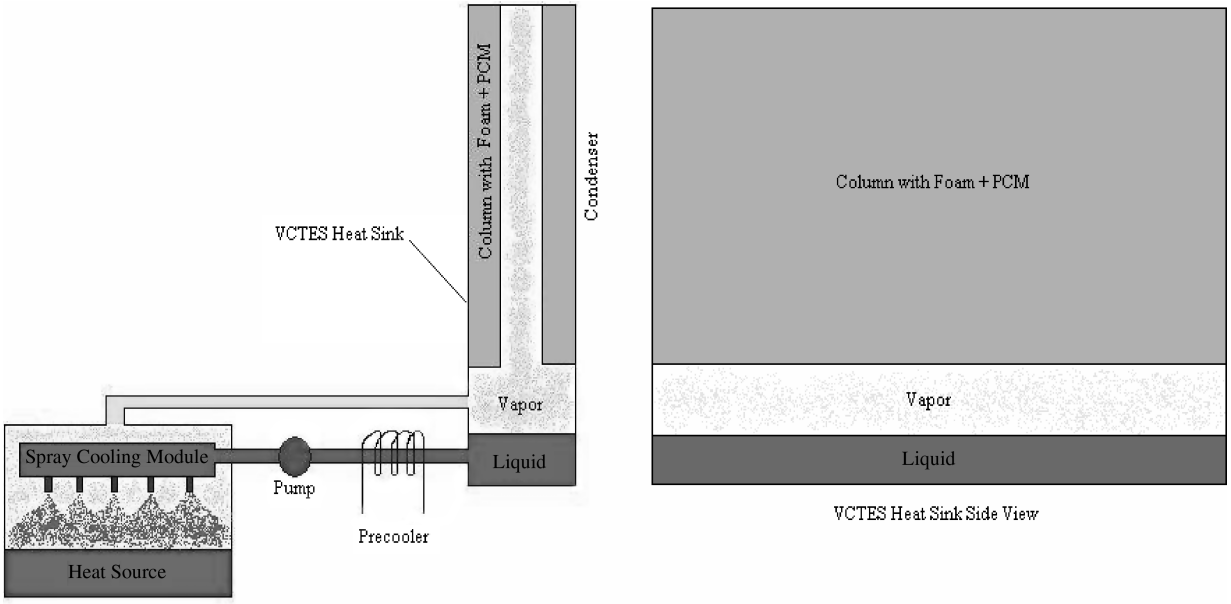

Fig. 1 Concept of integrated VCTES system (applied to a spray cooling module).

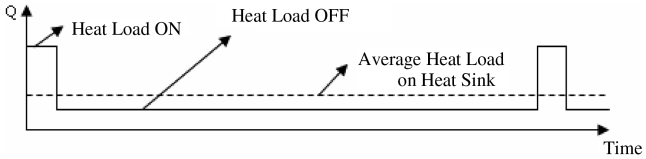

Fig. 2 Pulsated heat load diagram.

container. Once the vapor contacts the cold surfaces of the columns, it condenses and the PCM inside the columns absorbs the heat from the vapor and melts. The condensate then drips down because of gravity. When the heat load is off, the encapsulated phase change material (EPCM) refreezes by conducting heat laterally through the VCTES walls, which make up the condenser portion of the vapor chamber, and then the heat gets discharged to the ambient air (the surface that rejects heat to the air is termed as condenser in the paper because the inner side of the same surface acts as a condenser if no PCM columns were present, as in a normal vapor chamber). This process of charging during the heat-on time and discharging during the heat-off time repeats periodically over the thermal duty cycle (Fig. 2).

As shown in Fig. 2, the heat-off periods can also be periods of low heat loads. Because the PCM is saturated at the end of the heat-on time and has to discharge heat during the heat-off time, it cannot absorb any more heat (because most/all of it is in liquid phase). The condenser surface lying between the columns will directly participate in such applications and will discharge the small nonpeak period heat to the ambient air. In such cases, the columns can also carry a greater amount of PCM than needed to absorb the nonpeak period heat.

A key advantage of this design comes from using liquid–vapor phase change for heat absorption and using solid–liquid phase change as an intermediate condenser, unlike most heat sinks in which either one of PCM or a heat pipe is directly used to absorb and dissipate heat. Because liquid–vapor phase change is much faster compared with diffusion in a PCM, it is advantageous to first absorb pulse heat from the heat source rapidly using liquid–vapor phase change and then transfer it to PCM. The use of PCM as a second latent heat sink helps reduce the size of a condenser that would otherwise consist simply of a metal plate closing the vapor chamber (on the thermally opposite side of the heat source). For high heat fluxes (on the order of 500 W/cm^2), the size of a condenser plate can be very large, increasing the heat sink size. An intermediate sink in the form of PCM significantly helps in the reduction of the condenser size.

The following subsections outline the key design considerations used to arrive at a final design for the VCTES system that needs to be optimized.

A. Shape of the Containers for Thermal Energy Storage

Three types of shapes were considered for containers encapsulating the PCM: spherical, cylindrical, and cuboidal. Table 1 provides a comparison of the three shapes for choosing the best one for TES.

From Table 1 it can be seen that, although spherical[††] TES is available off the shelf and both spherical and cylindrical shapes provide for low heat flux requirements to the TES (owing to their increased surface area to volume ratio compared with cuboidal containers), they have a plethora of disadvantages with regards to key thermal performance parameters, such as heat absorption time, thermal resistance, easiness of using foam, vapor flow resistance, heat discharging path, and aiding the condenser performance by providing fins as extensions of the columns themselves. Though the cylindrical shape is reasonably competitive with cuboidal shape, the biggest disadvantage of using the cylindrical shape for the TES containers is having the foam cut in the cylindrical shape. This is a hassle and expensive as commercially available graphite foam is mostly in cuboidal shape.[‡‡] In addition, using cylindrical foam pieces in TES will increase the thermal contact resistance because it is difficult to cut and match the circular contour of foam with the inside of a cylindrical TES container. This is especially true if custom spherical containers are intended to be made. Cuboidal containers also provide for a low thermal resistance and low charging time [18] because, for the same surface area as a sphere or cylinder, a cuboid has the least distance from its circumference/perimeter to the center. Therefore, a cuboid is the optimum shape for TES storage containers.

B. Choice of Phase Change Material

Table 2 provides a comparison of various available phase change materials and their features and properties. To have a reasonable benefit of using the PCM for temporary energy storage, the sensible heat amount must be limited by limiting the temperature rise (equivalent to a small melting range). The vapor temperature inside the vapor chamber depends on the melting range of the PCM. Smaller

[††]Data available online. See Colvin, D. P., "Encapsulated Phase Change Materials," http://www.deltathermal.com/technology.htm [retrieved 19 July 2008].

[‡‡]Data available online at http://www.pocographiteonline.com/servlet/Categories?category=Thermal+Materials [retrieved 18 July 2008].

Table 1 Comparison of different shapes for TES containers

	Spherical	Cylindrical	Cuboidal
Commercial availability	Yes	Yes	No
Manufacturability	Easy	Moderate	Moderate
Heat absorption time	High	Moderate	Low
Thermal resistance	High	Moderate	Low
Incorporation of foam in TES	Difficult	Moderate	Easy
Vapor flow resistance	High	Low	Low
Improve condenser performance during discharging by providing column extensions as fins	No	Yes	Yes
Heat flux on each container	Low	Moderate	Moderate
Good heat discharging path	No	Moderate	Yes

Table 2 PCM comparison

	Organic paraffins	Metal/salt hydrates	Fatty acids	Organic–Inorganic eutectics	Glucose isomers
Heat of fusion, kJ/kg	220–300	170–340	20–50	200–500	185[a]
Density, kg/m^3	800–970	900–2200	800–900	1200–1800	1500–1600
Thermal conductivity, $W/m \cdot K$	~0.2	0.6–1.2	——	——	——
Thermal expansion	Medium to high	Low	High	High	——
Congruent melt	Yes	Mostly no	No	No	——
Supercooling	No	High	——	High	Low
Melting range	Mostly yes	No	——	——	——
Corrosiveness	Low	High	Mild	Mild	——
Toxicity	No	High	Mild	Mild	No

[a]Depends on the rate of heating

melting ranges help the PCM latent heat effect compete with the TES system sensible heat. Other than pure paraffins, most organic phase change materials have heating history dependent properties with a melting temperature range and undergo incongruent melting. Some of them even exhibit supercooling tendencies like inorganic salt hydrates.

From Table 2, it can be observed that both salt hydrates and pure paraffin waxes (with a narrow melting range) are the potential candidates for use in the VCTES system. The right choice of PCM depends on the experimental conditions and the selection of the HTF.

C. Selection of Heat Transfer Fluid

In the current heat sink design, fast heat absorption from a source is possible because of the phase change of the HTF, unlike in some heat sink designs in which the TES itself acts as the primary heat sink. The heat absorption rate would be very slow in such sinks because of the poor thermal conductivities of most of the available solid–liquid phase change materials. Therefore, the selection of the right HTF in the current heat sink is crucial. Any liquid–vapor phase change material with a high latent heat would be the ideal choice. Water can be used as the working fluid in the system because it has a high value of latent heat vaporization and will completely eliminate the risk of working with hazardous fluids in the vapor chamber. It will also reduce the cost.

III. Preliminary Mathematical Model

The VCTES system concept is optimized using a network-based resistance analysis. This simple mathematical model serves as a first design step and is not only useful in arriving at a fast prototype design for the experiments but also in filtering out the most important phenomena that need detailed numerical attention. The VCTES system operation broadly includes the following five functioning subprocesses: 1) depending on the application, the boiling or evaporation of the HTF on the heater surface producing vapor; 2) the flow of vapor onto a column bundle, 3) vertical film condensation on columns and, simultaneously, 4) the EPCM phase change/melting inside the columns, and 5) the EPCM freezing by conduction through the vapor chamber walls to the condenser

These processes can be characterized by a group of resistances signifying the heat charging and discharging modes as follows:

$R1$: vaporization/boiling resistance
$R2$: vapor–condensate interfacial resistance
$R3$: condensate film resistance
$R4$: column wall resistance (lateral direction)
$R5$: PCM conduction resistance without foam
$R6$: PCM conduction resistance without foam (same as $R5$)
$R7$: vapor chamber plate conduction resistance (along the thickness in the lateral direction)
$R8$: convective resistance of the condenser
$R9$: contact resistance in the air gap between the column wall and foam
$R10$: conduction resistance in the bond between the column wall and foam
$R11$: PCM conduction resistance with foam

The assumption made for this model is that, when the time is large, all the processes can be approximated as steady. Because the time is large at the end of the charging mode compared with any other instance during charging, the Fourier number will be large, which implies that heat conduction in any of the aforementioned processes will be large compared with the heat stored. Therefore, the thermal energy storage can be neglected and a resistance can be used to define the process. The case for processes during the discharging mode is similar. In addition, at any time instant, the system can be assumed to be in an instantaneous steady state. Even though this model is approximate, it serves as a fast design tool for preliminary design purposes. Figure 3 shows the heat sink schematic in terms of the dimensional variables. Figure 4 shows the resistance paths for the two modes of operation of the VCTES system. A single column geometry showing the dimensional variables is shown in Fig. 5. It must be noted that, in defining some of the resistances, the dimension $(z + t_{\text{wall}})$ is approximated as z for simplicity. This is true because of the fact that $z \gg t_{\text{wall}}$ or t_c in the design.

In the aforementioned model, $R1$ is evaluated depending on the intended application and the mode of heat removal at the heater surface, which can be, for example, pool boiling or spray cooling. $R2$ is evaluated using the Maxwell velocity distribution for vapor from the kinetic theory of gases, which helps determine the flux of molecules passing through the vapor–condensate interface. Knowing the mass flux and latent heat, the heat flux to the

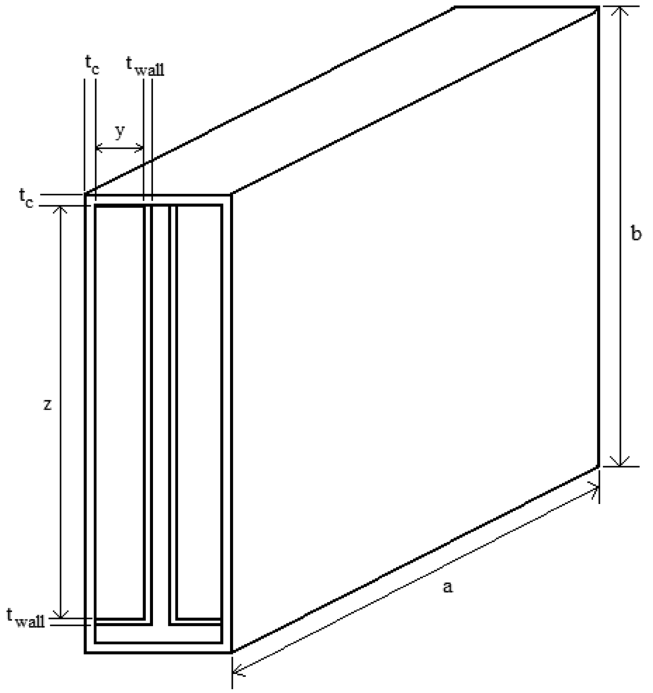

Fig. 3 VCTES schematic showing dimensional design variables.

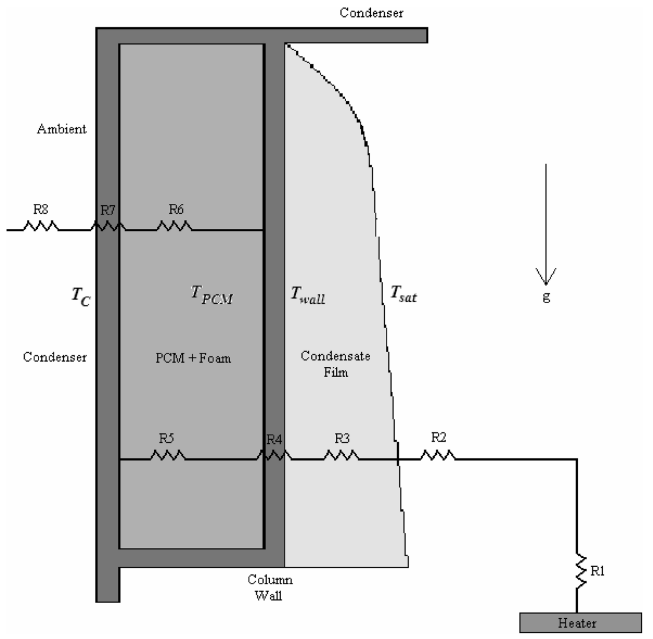

Fig. 4 VCTES charging and discharging paths.

interface can be evaluated; this was used to get the interfacial resistance $R2$ as

$$R2 = \left(\left(\frac{2\sigma \cdot x \cdot z}{2-\sigma}\right)\left(\frac{h_{\mathrm{lv}}^2}{T_{\mathrm{sat}} v_{\mathrm{lv}}}\right)\left(\frac{M}{2\pi R_u T_{\mathrm{sat}}}\right)^{\frac{1}{2}}\left(1-\frac{P_{\mathrm{sat}} v_{\mathrm{lv}}}{2h_{\mathrm{lv}}}\right)\right)^{-1} \quad (1)$$

A detailed explanation of this procedure is presented in [19]. An accommodation coefficient of 0.03 was used in the calculations, which is a typical value for water. Knowing $R2$ helps determine whether the vapor side temperature boundary condition for the film condensation is T_{sat} or if there is a drop at the liquid–vapor interface because of vapor flow.

$R3$ is calculated from the Nusselt theory [19] for steady laminar film condensation on a vertical wall as follows:

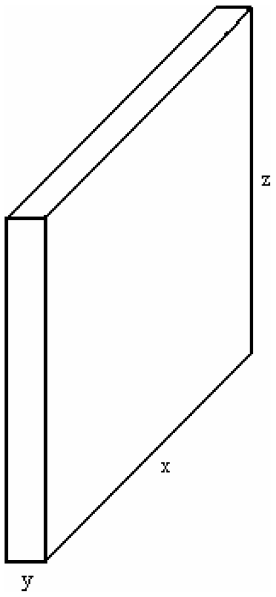

Fig. 5 Geometry of a single TES column inside the VCTES heat sink.

$$R3 = \left(\frac{0.79x^4 z^3 g\rho_l(\rho_l-\rho_v)k_l^3 h_{\mathrm{lv}}}{\mu_l(T_{\mathrm{sat}}-T_{\mathrm{wall}})}\right)^{-0.25} \quad (2)$$

All the resistances, $R4$–$R11$, except $R8$ were calculated assuming pure conduction and were evaluated accordingly as per the geometry as follows:

$$R4 = \frac{t_{\mathrm{wall}}}{k_{\mathrm{wall}} xz}, \qquad R5 = \frac{y}{k_{\mathrm{PCM}} xz}, \qquad R7 = \frac{t_c}{k_c xz}$$
$$R9 = \frac{t_{\mathrm{air}}}{k_{\mathrm{air}} xz}, \qquad R10 = \frac{t_b}{k_b xz}, \qquad R11 = \frac{y}{k_{\mathrm{eff}} xz} \quad (3)$$

$$k_{\mathrm{eff}} = k_{\mathrm{foam}}(1-\varepsilon) + k_{\mathrm{PCM}}\varepsilon \quad (4)$$

Natural convection in the melt can be neglected for PCM phase change in foams because of a very low Rayleigh number. This is because of an increased capillary effect and, hence, a reduced gravity effect in foams along with a low temperature difference between the foam ligament and PCM for graphite foams. It is shown in [20] that, for foams with surface area to volume ratios of more than 1575 $(\mathrm{m}^2/\mathrm{m}^3)$, a single temperature representative of both the foam and PCM can be used.[§§] For carbon foams, this ratio is about 20,000 $(\mathrm{m}^2/\mathrm{m}^3)$[§§]; therefore, it is reasonable to assume foam and PCM as one composite material and use effective properties based on foam porosity to evaluate the conduction resistance $R11$.

The condenser side thermal resistance $R8$ is evaluated from the convective coefficient, which in turn depends on the requirement as dictated by the condenser side heat flux:

$$R8 = \left(\frac{xzq_C}{T_C - T_{\mathrm{air}}}\right)^{-1} \quad (5)$$

$$q_C = \frac{q_H D A_H}{nxz} \quad (6)$$

When finding the resistance values, a conservative approach is used wherever applicable. A detailed flowchart for the optimization of the mathematical model is shown in Fig. 6.

Thermophysical properties for saturated liquid and vapor need to be changed whenever P_{sat} and T_{sat} are changed in the process of iterative optimization because of varying other variables. At a point

[§§]Data available online. See Klett, J., "High Thermal Conductivity Graphite Foam," www.ms.ornl.gov/researchgroups/cmt/foam/foams.htm [retrieved 19 July 2008].

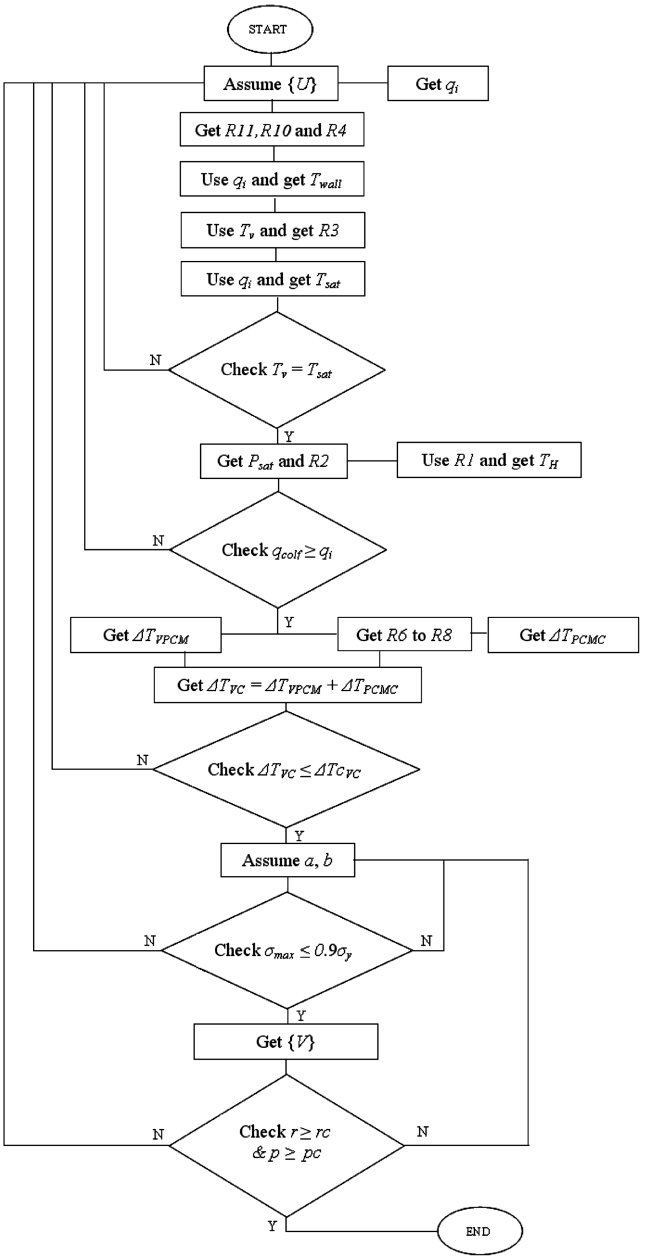

Fig. 6 Flowchart for the iterative optimization of the VCTES heat sink.

in the flowchart at which $\sigma_{\max}$ is checked with σ_y, if the condition fails, the first option would be to change/decrease a and/or b rather than going up all the way to the top of the chart. If the vapor chamber size (a and b) reaches a practical limiting value such that the number of columns of the size assumed in the guess set $\{U\}$ does not fit in it, then the appropriate column size values in $\{U\}$ are guessed again and the optimization is repeated. A similar methodology is employed at the last step of the optimization involving comparing r with rc and p with pc.

Even though a "no definitive condition" can be employed to stop the iterative optimization, the assumed critical values ΔTc_{VC}, rc, pc, and a reasonable value of m_{tot} would break the flowchart to arrive at a preliminary design. It must be noted that the higher the value of p is, the higher the latent advantage in the heat sink design is and hence the higher the storage densities are. A high value of r makes sure that all the PCM present in the system gets used in storing heat. Unused PCM does not contribute to the latent advantage of the heat sink but results in increasing the mass. Therefore, it is very important to achieve a balance between high p and high r in the system. It is very tempting to lower the parasitic mass of the heat sink by choosing very thin plates that make up the vapor chamber setup. However, it must be remembered that this leads to undesirable stress and deflection of the plates. If the stress developed in the plates that make up the heat sink exceeds the maximum value that the material with which they are made up of can take, then the plates fail. The reason for the plates to develop stress is the high internal pressures desired in the chamber for the working fluid; working fluid at high pressures will have a higher heat absorption capacity. Therefore, the failure of the plates will be under tension because of the high internal pressures in the chamber. This shows the importance of including the stress and deflection analysis in the optimization flowchart of Fig. 6. The result set $\{V\}$ consists of all the output terms of Fig. 6.

In Fig. 6, the variable and property data set U is first assumed and is defined as

$$\{U\} = [x, y, z, n, T_v, T_{\mathrm{PCM}}, \Delta Tc_{\mathrm{VC}}, rc, pc, \text{vapor chamber material}, \times \text{column material, foam material, and PCM}] \tag{7}$$

and q_{colf} is calculated as

$$q_{\mathrm{colf}} = \left[\frac{(T_{\mathrm{sat}} - T_{\mathrm{PCM}})}{R2 + R3 + R4 + R10 + R11}\right]\frac{1}{xz} \tag{8}$$

The parameter q_{colf} verifies whether a TES column is capable of absorbing the heat flux based on the surface area ratio between itself and the heater surface. If q_{colf} is less than q_i, it implies that the thermal resistance in transferring heat from the vapor to the TES container is large for the design; therefore, the container cannot absorb the heat that is desired, q_i, for absorption. In that case, the design parameters need to be modified.

IV. Results and Discussion

For illustration purposes, a heat source in an example application with a D of 0.05, generating a pulse load of 500 W/cm^2 over an area of 100 cm^2 has been considered. The surface temperature in this particular application should be kept between 100 and 135°C.

The preliminary mathematical model is used to optimize and arrive at a best configuration for an example heat sink for the considered application and is assumed to have to meet the following criteria simultaneously: a) critical temperature difference between vapor and condenser (ΔTc_{VC}) = 10 °C, b) critical value for the ratio of used PCM mass to the total PCM mass (rc) = 90% and of total PCM mass to total VCTES mass (pc) = 45%, c) low heat flux on the condenser portion, d) environment-safe operation, and e) fast charging ability.

A. Possible Solutions to Meet the Design Criteria of an Example Heat Sink

1) A minimum possible ΔT_{VC} ensures a narrow temperature range of operation of the VCTES system, which is very important. This is made possible by choosing a PCM with as narrow a melting range as possible and decreasing the values of all the resistances during charging and discharging, which in turn is made possible by any or some of the following methods:

a) The number of columns can be kept the same and, by increasing the column height (and thereby increasing the surface area of each column), the heat flux on each column can be decreased. But this increases the overall size and mass of the VCTES system. This also increases the used PCM amount and decreases resistance $R8$.

b) The column height and the amount of PCM can be kept the same. Increasing the length of each column decreases the width. This decreases the resistance $R11$ in the foam-filled PCM portion of each column. This also decreases the resistance $R8$.

c) The column size can be kept the same and by increasing the number of columns, the heat flux during charging can be decreased. But this increases the overall mass m_{tot} of the VCTES system (with most of the increase happening in the form of parasitic mass).

2) Though it is good for the VCTES system to have a high PCM mass to the VCTES system mass ratio, it is not appropriate to increase

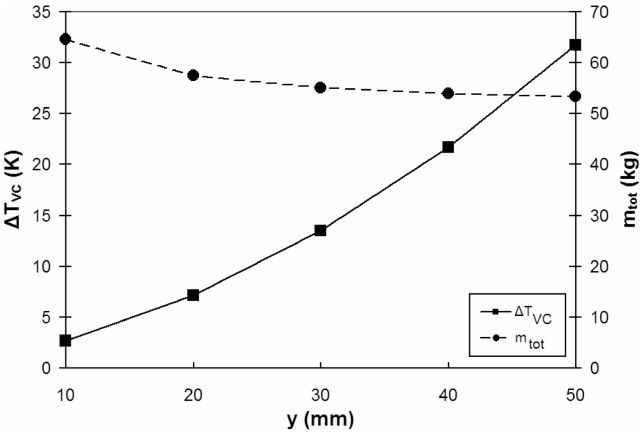

Fig. 7 Selection of optimized case for an example heat sink.

the amount of unused PCM just to increase this ratio. It is important to minimize the amount of excess PCM. Therefore, to achieve $r \geq rc$ is important, and this can be done by decreasing the TES size, which in turn affects all the resistances and mass.

3) Having a minimum possible heat flux on the condenser portion of the VCTES system is crucial during discharging mode. A lousy condenser may not dissipate the heat to the ambient air within the no-heat-load time. Because of this, the inside temperatures may increase and the VCTES system may not be ready for the next pulse of the cycle. The heat flux on the condenser can be decreased by increasing its surface area either by increasing the length or height of TES containers, both of which increase the mass. Depending on the application, if heat flux on the condenser turns out to be very high, fins can be provided on the condenser, which can simply be protrusions of columns inside the vapor chamber.

4) Accidental leakage of hazardous vapor chamber fluids can be environmentally unsafe, and so water is chosen as the HTF for this example heat sink.

5) Because the duty cycle for the example heat sink is low, fast charging is crucial. This can be achieved by minimizing the resistances $R1$–$R4$, $R10$, and $R11$.

B. Optimized Results

Based on the aforementioned constraints, the developed VCTES design code was run multiple times by varying the values of column width, length, and height. The results are shown in Fig. 7. For all the runs, the vapor chamber and column material was assumed as Titanium, the bond material (to bond foam to column inside surface) as S-bond®[¶¶], and the PCM as pure POLYWAX® 1000.[***]

From the result set, an optimized case was chosen, which satisfies the design criteria considered. For this optimization, because most of the guess values in the set $\{U\}$ are fixed by virtue of the assumed application, the only variable was column size (x, y, z). Even the column number was fixed a priori. Changing y such that there is always a minimum amount of PCM present in the system to absorb the heat generated will give values for x and z for each case. It can be observed from Fig. 7 that $y = 20$ mm is an optimum value for the width of the TES units because ΔT_{VC} for this case lies below $\Delta T c_{\text{VC}}$ and it satisfies all the other design criteria listed at the beginning of this section. The dimensions for the VCTES heat sink are shown in Table 3. Table 4 shows the thermal resistances during the charging and discharging modes for the heat sink in Table 3, and Table 5 shows some parameters of the result set $\{V\}$. A parallel optimization was done assuming the columns as cylindrical and it was observed that, by changing the column shape from cylindrical to cuboidal and keeping all other parameters exactly the same, there is scope for decreasing the unused PCM mass and even ΔT_{VC}. The importance of using foam inside the columns and using a thermal conductive bond between the foam and column inside surface (which is otherwise occupied by air or PCM or both) can also be observed from Table 3.

Table 3 Example VCTES heat sink optimized design parameters

Parameter	Value
a, m	1.006
b, m	1.001
tc, mm	0.4
N	2
x, m	1
z, m	1
y, mm	20
t_{wall}, mm	0.4
q_i, W/cm^2	2.5
q_{colf}, W/cm^2	2.5
T_{sat}, K	393
P_{sat}, atm	1.95
T_C, K	385.9
q_C, W/cm^2	0.1
ΔT_{VPCM}, K	6.9
ΔT_{PCMC}, K	0.1
t, s	140

Table 4 Thermal resistances of the example VCTES heat sink

Resistance, K/kW	Value
$R1$	0.34
$R2$	0
$R3$	0.1
$R4$	0.03
$R5$	133
$R8$	79
$R9$	1
$R10$	0
$R11$	0.15

Table 5 Key parameter values of the result set $\{V\}$

Key Result	Value
ΔT_{VC}, K	7
m_{PCM}, kg	27
V_{tot}, m^3	0.072
m_{tot}, kg	57.5
r	97.5
p	47
Q, MJ	7
Q_v, MJ/m^3	97
Q_m, kJ/kg	122

C. Discussion of the Preliminary Design

From the results, it can be observed that, during charging mode, the dominant resistance to heat transfer is from the PCM ($R5$) unless there is foam. With the presence of foam, $R2$ and $R4$ can be neglected compared with $R1$, $R3$, and $R11$. A high value of $R9$ suggests that it is essential to use a thermal conductive bond to attach foam to the column inner walls. During the discharging mode, the dominant resistances are again $R6$ and $R8$ unless there is foam and a bond, and then the conclusion is same as the charging mode. With the presence of foam, all the resistances can be neglected compared with $R8$. These observations provide good support to the intuitive design features assumed. A point of interest that needs to be mentioned is that, with such low resistance values, the selection of a highly thermal conductive material for the vapor chamber and column plates

[¶¶]Data available online at http://www.s-bond.com/pdfs/Prop_-Bull_SB220.pdf [retrieved 18 July 2008].

[***]Data available online at http://www.bakerhughesdirect.com/cgi-bin/bpc/myHomePage/myHomePage.jsp [retrieved 18 July 2008].

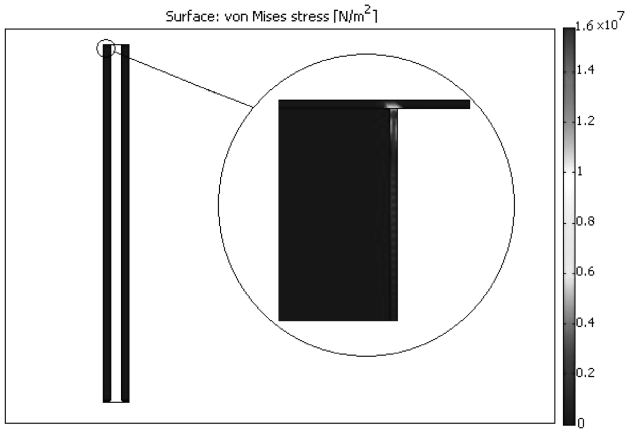

Fig. 8 Stress distribution in the VCTES heat sink.

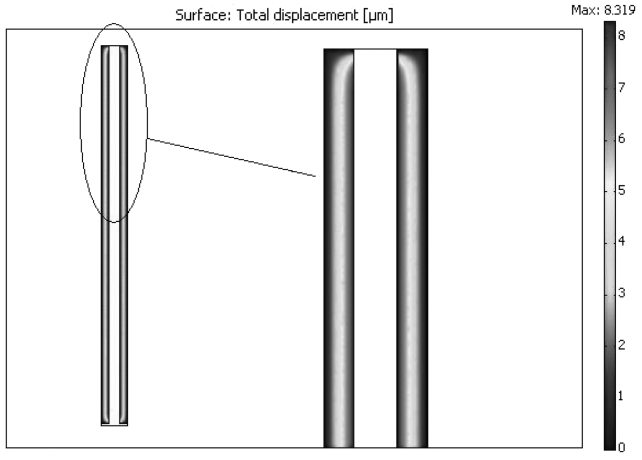

Fig. 9 Deflection of TES column plates for $P = 1.95$ atm.

becomes unimportant. This was verified by using copper as the material everywhere. It was found that copper increases the weight but does not help significantly in reducing the ΔT_{VC}.

To execute the step in the flowchart at which the design is checked for structural failure, a two-dimensional model of the VCTES heat sink is analyzed for stress using a commercial FEM package, COMSOL® [21]. The results are shown in Figs. 8 and 9. From Fig. 8, it can be seen that a σ_{max} of 16 MPa is developed at the column and vapor chamber wall interface, which is much lower than the tensile yield strength of pure titanium or any of its alloys. The stress developed in graphite foam is found to be less than 3 MPa (compressive strength of Pocofoam®)[†††] , and so the foam does not fail/crumble. The maximum deflection of the column walls can be seen in Fig. 9, which is 8.3 μm and is a very low number compared with the TES lateral dimension y. As assumed before, TES columns are able to provide support to the vapor chamber plates and the foam was able to support the TES column plates.

In addition to providing scope for a preliminary design, the order of magnitude analysis of the resistances helps in isolating the key processes of the VCTES heat sink operation that require detailed numerical attention. For example, from Table 3 it can be inferred that film condensation on the outside of a column wall coupled with the simultaneous phase change of PCM in foam inside the column is a crucial hindrance for fast charging. During discharging, it is the heat dissipation to the ambient air that causes a delay.

The design described in Table 3 has a volumetric heat storage capacity of 97 MJ/m^3. This was made possible because by assuming an isothermal melting point for PCM. If the PCM melting range is considered (90–120°C for POLYWAX® 1000) and if the VCTES system operates within the melting range of the PCM, then Q and hence the volumetric heat storage both reduce. The effect of operating within the PCM melting range on the volumetric heat storage capability as applicable to the current optimized design is shown in Fig. 10. It can be seen that, for PCM with a melting range, the volumetric heat storage capacity is proportional to the operating temperature range of the heat sink within the melting range of the PCM. This is because the wider the operating temperature range within the melting range of a PCM is, the greater the latent heat effect is, which accounts for more volumetric storage.

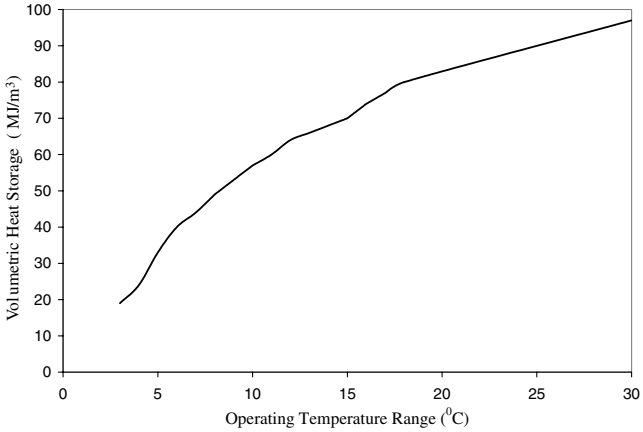

Fig. 10 Volumetric heat storage capacity vs operating temperature range of the VCTES system.

V. Conclusions

A novel concept for a heat sink has been proposed. Key design considerations for selecting the best features for the concept were mentioned. A preliminary model has been developed and is useful in isolating the important processes that need detailed numerical attention. The model also serves as a fast design tool for prototype development and experimentation.

It is shown that it is possible to have a heat sink with attractive features such as a high heat storage ability (7 MJ), compactness (0.072 m^3, 57.5 kg), a low vapor-to-condenser temperature difference (7°C), a fast charging ability, environment-safe operation, a high heat flux capability (500 W/cm^2 over an area of 100 cm^2), and a high energy storage density (97 MJ/m^3, 0.122 MJ/kg), including added features of a vapor chamber such as self-acting and quiet operation.

The promising aspects that make this concept feasible include using carbon foam in the TES columns (which help the thermal conductivity of TES increase from ~0.2 W/(m · K) to 135 W/(m · K) for Pocofoam®[†††] and 245 W/(m.K) for PocoHTC®[‡‡‡]), a large surface area for TES (which helps in fast charging/heat absorption and a low heat flux at each column, thus reducing the temperature gradients), and placing PCM containers inside the vapor space of the chamber to ensure rapid transport of pulse heat loads to the PCM containers. The mathematical model described is an approximate theoretical model and is only a guideline to estimate the thermal performance and feasibility of the concept but is not a thorough final design criterion. Detailed in-depth numerical analysis and experiments are to be performed to understand and accurately quantify the key processes that govern VCTES heat sink performance during transient operation.

Acknowledgment

The authors wish to sincerely thank Michele Puterbaugh, the program manager at Universal Technology Corporation, Dayton, Ohio, for funding the work.

[†††]Data available online at http://www.poco.com/tabid/130/Default.aspx [retrieved 5 August 2008].

[‡‡‡]Data available online at http://www.poco.com/tabid/127/Default.aspx [retrieved 5 August 2008].

References

[1] Chow, L. C., Zhong, J. K., and Beam, J. E., "Thermal Conductivity Enhancement for Phase Change Storage Media," *International Communications in Heat and Mass Transfer*, Vol. 23, No. 1, 1996, pp. 91–100. doi:10.1016/0735-1933(95)00087-9

[2] Gallego, N. C., and Klett, J. W., "Carbon Foams for Thermal Management," *Carbon*, Vol. 41, No. 7, 2003, pp. 1461–1466. doi:10.1016/S0008-6223(03)00091-5

[3] Chang, M., Chow, L. C., Chang, W. S., and Morgan, M. J., "Transient Behavior of Axially Grooved Heat Pipes with Thermal Energy Storage," *Journal of Thermophysics and Heat Transfer*, Vol. 6, No. 2, 1992, pp. 364–370. doi:10.2514/3.368

[4] Weislogel, M. M., "Heat and Mass Transfer in a Dual-Latent Thermal Energy Storage System," M.S. Thesis, Dept. of Mechanical and Materials Engineering, Washington State Univ., 1988.

[5] Weislogel, M. M., and Chung, J. N., "Experimental Investigation of Condensation Heat Transfer in Small Arrays of PCM-Filled Spheres," *International Journal of Heat and Mass Transfer*, Vol. 34, No. 1, 1991, pp. 31–45. doi:10.1016/0017-9310(91)90170-J

[6] Horbaniuc, B., Dumitrascu, G., and Popescu, A., "Mathematical Models for the Study of Solidification Within a Longitudinally Finned Heat Pipe Latent Heat Thermal Storage System," *Energy Conversion and Management*, Vol. 40, Nos. 15–16, Oct. 1999, pp. 1765–1774. doi:10.1016/S0196-8904(99)00069-2

[7] Liu, Z., Wang, Z., and Ma, C., "An Experimental Study on Heat Transfer Characteristics of Heat Pipe Heat Exchanger with Latent Heat Storage. Part I: Charging Only and Discharging Only Modes," *Energy Conversion and Management*, Vol. 47, Nos. 7–8, May 2006, pp. 944–966. doi:10.1016/j.enconman.2005.06.004

[8] Liu, Z., Wang, Z., and Ma, C., "An Experimental Study on Heat Transfer Characteristics of Heat Pipe Heat Exchanger with Latent Heat Storage. Part II: Simultaneous Charging/Discharging Modes," *Energy Conversion and Management*, Vol. 47, Nos. 7–8, May 2006, pp. 967–991. doi:10.1016/j.enconman.2005.06.007

[9] Cogliano, J. A., W.R. Grace & Co., New York, U.S. Patent for a "Passive Solar Heating and Cooling Panels," Patent No. 4,273,100, 16 June 1981.

[10] Basiulis, A., Hughes Aircraft Co., Los Angeles, U.S. Patent for a "Rechargeable Thermal Control System," Patent No. 4,673,030, 16 June 1987.

[11] Cao, Y., Miami, FL, U.S. Patent for a "Human Body Cooling Suit with Heat Pipe Transfer," Patent No. 5,386,701, 7 Feb. 1995.

[12] Giammaruti, R. J., Hudson Products Corp., Houston, TX, U.S. Patent for a "Passive Cooling of Enclosures Using Heat Pipes," Patent No. 5,579,830, 3 Dec. 1996.

[13] Glover, R. J., Bishop, M. R., and Tenser, M. S., Nortel Networks Corp., Montreal, U.S. Patent for a "Packaging System for Thermally Controlling the Temperature of Electronic Equipment," Patent No. 6,104,611, 15 Aug. 2000.

[14] Lin, L., Leland, J. E., and Ponnappan, R., The United States of America as Represented by the Secretary of the Air Force, Washington, DC, U.S. Patent for a "Cooling of Electro Mechanical Actuator with Phase Change Material and Thermosyphons Containing Working Fluid," Patent No. 6,294,853 B1, 25 Sept. 2001.

[15] Kung, S., and Liu, C., Compal Electronics, Inc., Taipei, Taiwan, U.S. Patent for a "Thermal Module with Temporary Heat Storage," Patent No. 6,971,443 B2, 6 Dec. 2005.

[16] Zuo, J., and Ernst, D. M., Thermal Corp., Stanton, DE, U.S. Patent for a "Heat Pipe Having a Wick Structure Containing Phase Change Materials," Patent No. 6,889,755 B2, 10 May 2005.

[17] Liu, Z., Wang, Z., Sun, X., Li, J., and Ma, C., Chinese Patent for "A Multifunctional Heat Pipe Exchanger with Latent Heat Storage," Patent No. 03242284.9, 2006.

[18] Zivkovic, B., Fujii, I., "An Analysis of Isothermal Phase Change of Phase Change Material Within Rectangular and Cylindrical Containers," *Solar Energy*, Vol. 70, No. 1, 2001, pp. 51–61. doi:10.1016/S0038-092X(00)00112-2

[19] Carey, V. P., *Liquid-Vapor Phase-Change Phenomena*, 1st ed., Taylor and Francis, Oxford, 1992.

[20] Du, J., Chow, L., and Leland, Q., "Optimization of High Heat Flux Thermal Energy Storage with Phase Change Materials," American Society of Mechanical Engineers, Paper IMECE2005-80327, 2005.

[21] COMSOL Multiphysics, Modeling Package, Ver. 3.3, COMSOL, Inc., Burlington, MA, 1997–2007.